Adaptive Trigger Delay Using a Predictive Model Applied to Black Blood Fast Spin Echo Cardiac Imaging in Systole

B. Fernandez[1,2], J. Oster[2,3], M. Lohezic[1,2], D. Mandry[2,4], O. Pietquin[2,5], P-A. Vuissoz[2,3], and J. Felblinger[2,3]

[1]Global Applied Science Lab., GE Healthcare, Nancy, France, [2]IADI, Nancy-Université, Nancy, France, [3]U947, INSERM, Nancy, France, [4]CHU de Nancy, Nancy, France, [5]IMS Research Group, Supelec Metz Campus, Metz, France

Introduction: In clinical applications, cardiac gated sequences are commonly used for heart imaging. In practice, we simply wait a fixed time called Trigger Delay (TD) after the R-wave has been detected to acquire data in the chosen cardiac phase. The main problem of this method is that the TD is constant and does not take into account the physiological variability such as instantaneous heart rate changes during breath-hold or free breathing. Another issue is that we cannot use a TD shorter than the preparation time. Consequently when a cardiac gated sequence with a long preparation time is used, only diastolic images are achievable. Double Inversion Recovery Fast Spin Echo (DIR-FSE), resulting in black-blood images of the heart [1], is such a sequence since the inversion time (TI) needed to cancel the blood signal is around 500ms. Systolic view of the heart could also be of clinical interest, especially during end-systolic phase when the cardiac volume is minimum and constant (average TD = 300ms, average duration 60ms [2]). The primary aim of this work was to assess a robust method to acquire black blood FSE in end-systolic phase. For this purpose, the DIR preparation has to be launched before the R-wave in the previous cardiac cycle. A RR interval prediction is then needed and heart rate variability has to be accounted in order to position the acquisition window properly. A new general adaptive method is described here that overcomes the above listed limitations in prospectively cardiac gated sequences with long preparation time using a predictive model. This method has been applied on end-systolic black blood FSE images.

Materials and Methods:

Prediction: To launch the DIR preparation before the R-wave, the method described in [3] has been used. A Kalman filter [4] is implemented to make a one-step prediction of the R-R interval duration (ΔT_{RR}). Since the instantaneous heart rate is known to change with respiration [2], several inputs are used: the past $\Delta T_{RR}(n-1), \Delta T_{RR}(n-2)$, a respiratory belt and its derivative sampled at R-wave times to predict $\Delta\hat{T}_{RR}(n)$.

Model: To take into account instantaneous heart rate variability, a model of the cardiac cycle, previously described in [5], was used. This model gives the length of the systole (ΔTs) and the length of the diastole (ΔTd) based on instantaneous heart rate. The Kalman filter described in [3] was extended to a two-step prediction by modifying the state model of the Kalman filter [4]. As a result, at time t_n, the time when the next cardiac cycle begins ($t_n + \Delta\hat{T}_{RR}(n)$) and its duration ($\Delta\hat{T}_{RR}(n+1)$) can be predicted. Duration of the next systole (ΔTs) and end-systolic phase can be predicted and an optimal TD $\hat{T}Dopt(n+1)$ is computed (Figure 2). The delay $\hat{D}$ between the last detected R wave and the beginning of the DIR preparation is then deducted from $\hat{T}Dopt(n+1)$ and from the fixed TI (Figure 1).

Implementation: Signals from respiratory belt and ECG sensors were transmitted from a custom Maglife (Schiller Medical, Wissenbourg, France) monitoring system to a dedicated home built real time electronic hardware presented in [6]. Every computation, such as R-wave detection and Kalman filtering, are made in real-time on our home built system. A TTL output of the real-time system is plugged into the external trigger input of the scanner hardware (1.5T Signa HDx, GE Healthcare, Milwaukee, WI) and is used to launch the sequence. The system works as follow: when an R-wave is detected, the Kalman filter is updated and $\hat{T}Dopt$ and $\hat{D}$ are computed based on predicted R-R interval durations. $\Delta\hat{T}_{RR}(n+1)$ is used to compute the adaptive optimal TD $\hat{T}Dopt(n+1)$, the delay $\hat{D}$ is computed based on $\Delta\hat{T}_{RR}(n)$, $\hat{T}Dopt(n+1)$ and TI (Figure 2). After the delay $\hat{D}$, the DIR preparation is played out.

Experiment: This method has been applied to four healthy volunteers (age: 35.5±12 y., weight: 75±10 kg.). For each volunteer, two short-axis images in end-systolic phase in breath-hold were acquired using the DIR-FSE sequence: the first image used the proposed method and the second image used a fixed TD. In the latter case, TD was computed based on the average heart rate ($\overline{\Delta T_{RR}}$) and the corresponding $\overline{\Delta Ts}$ according to the cardiac cycle model [5], i.e. $TD = \overline{\Delta T_{RR}} - TI + \overline{\Delta Ts} - T_a$. (See Figure 2, TD=650ms for an average heart rate of 70 bpm). A conventional cine balanced-SSFP sequence with high temporal resolution was also acquired in the same plane and considered as the reference to depict end-systolic phase. Parameters for the DIR-FSE were TE=20ms, TI=500ms, BW=125kHz, ETL=16, matrix size=256x256. The corresponding T_a in Figure 2 was 100ms.

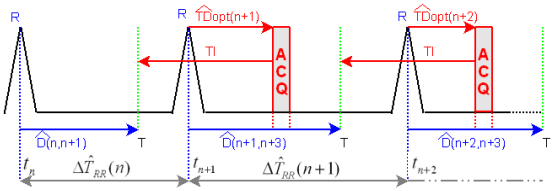

Figure 1: Timing of the suggested method for adaptive systolic DIR-FSE.

$$\Delta\hat{T}s(n+1) = 546 - 2.1\times H\hat{R}_t \text{ with } H\hat{R}_t = \frac{60}{\Delta\hat{T}_{RR}(n+1)\times 10^{-3}}$$

$$\hat{T}Dopt(n+1) = \Delta\hat{T}s(n+1) - T_a$$

$$\hat{D}(n,n+1) = \Delta\hat{T}_{RR}(n) - TI + \hat{T}Dopt(n+1)$$

Figure 2: Formulas for the computation of the adaptive trigger times. T_a is the time needed to perform the FSE sequence (excluding DIR preparation). All values are given in ms except $H\hat{R}_t$ (bpm).

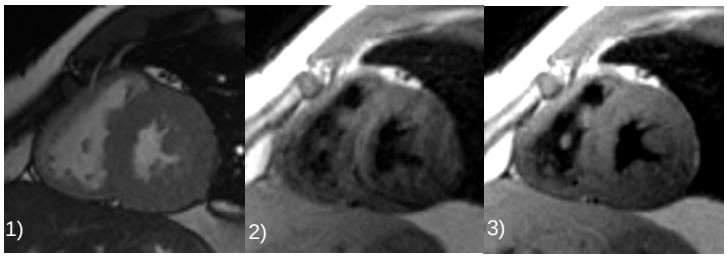

Figure 3: Results obtained on Volunteer 1. 1) systolic image from the CINE, 2) conventional DIR-FSE with a fixed TD, 3) our suggested method.

	Fixed TD				Optimal TD			
Vol.	HR	Error	MSE	Mark	HR	Error	MSE	Mark
1	70	227±71	59	0	85	1±38	9	2
2	72	80±31	21	1	72	-4±29	7	2
3	59	163±54	41	0	56	-8±31	8	2
4	55	-5±44	10	2	58	-4±26	6	2

Table 1: Results obtained on four volunteers (Vol.). HR (bpm) is the average heart-rate during acquisition, the error done on TD compared to the ideal TD computed retrospectively is given in average (ms) ± standard deviation (ms) and MSE (ms) is the mean squared error. Mark referred to the image quality assessed by the radiologist (0=Unusable, 1=Usable but with artifact, 2=Usable, artifacts free).

Results and Discussion: This method was successfully applied to all volunteers. Figure 3 shows a typical example from Volunteer 1. Table 1 displays the error done compared to the ideal adaptive TD computed retrospectively and the image quality assessed by a radiologist with experience in cardiac MRI. As shown in Figure 3, this technique can reliably position DIR preparation, and consequently acquisition window, to acquire end-systolic black-blood FSE images despite physiological variability. These images would be helpful in depicting heart wall details, such as fatty infiltration of the right ventricle wall occurring in arrythmogenic right ventricular cardiomyopathy. Results demonstrates the robustness of this adaptive method for end-systolic DIR-FSE. However, generalization to any ECG-gated sequence, or to any cardiac phase is straight-forward. Moreover, this method can be used in apnea or free breathing since the respiratory variability is managed by the Kalman filter. A limitation of this method is through-plane motion as the DIR preparation are applied in diastole whereas data acquisition is performed in systole. To handle this problem, the thickness of selective IR has been made slightly larger than the slice thickness but a method such as [7] should give better results. Thanks to these preliminary results, this method will be tested on a large patient population to assess its robustness and clinical interest.

References: [1] Simonetti *et al.*, Radiology 199, 49-57 (1996) [2] Libby *et al.*, Braunwald's Heart Disease, 8th Edition, Elsevier (2008) [3] Oster *et al.*, ICASSP 513-516 (2008) [4] Kalman, ASME-JBE 82, 35-45 (1960) [5] Bacharach *et al.*, JNM 31, 38-42 (1990) [6] Odille *et al.*, IEEE-TBME 54 630-640 (2007) [7] Keegan *et al.*, JMRI 24 563-570 (2006).